Experimental investigation on through-wall imaging based on non-linear inversions

Qingyang Meng, Dexin Ye, Jiangtao Huangfu, Changzhi Li and Lixin Ran✉

Through-wall imaging (TWI) is a challenging topic in the area of inverse scattering problem based microwave imaging. A TWI solution based on non-linear inversion algorithms is experimentally investigated. Experiments are performed using a setup with the object surrounded by a closed wall. The inversion is based on a twofold subspace-based optimisation method, and the results show that the location, shape, size, and dielectric constant of the object can be successfully retrieved from the measured scattering data. This is the first experimental demonstration of TWI of objects behind a closed wall using a non-linear inversion algorithm. These results imply the potential of TWI for practical applications.

Introduction: Microwave through-wall imaging (TWI) is a challenging technique aiming to detect the geometric and dielectric parameters of targets behind obstacles. It can be potentially used in areas such as non-destructive diagnosis, rescue, and medical imaging [1]. As an important aspect of microwave imaging, it has attracted many interests.

So far, TWI researches based on different algorithms and regularisation schemes have been reported. Examples include the truncated singular value decomposition inversion scheme with linear Born model [2], the contrast source inversion algorithm (CSI) [3], and the finite-difference (FD) based approaches such as FD-CSI [4]. The effectiveness of these methods has been demonstrated by numerical examples. However, experimental verifications are rarely reported, especially for TWIs with closed walls and non-linear inversion algorithms.

In this Letter, we experimentally investigate the TWI based on non-linear inversion algorithms. Experiments are conducted using a setup with the object surrounded by a closed wall. The inversion is based on a non-linear approach, aiming to retrieve the location, shape, size, and dielectric constant of the object from the measured scattering data. To the best of our knowledge, this is the first experimental demonstration of TWI of objects behind a closed wall using a non-linear inversion algorithm.

Algorithm: Among many non-linear inversion algorithms, in this work, we adopt the twofold subspace-based optimisation method (TSOM), which is robust against noises [5]. This is important for experimental data. The inversion is based on equations

$$\bar{E}^{\mathrm{sca}} = \bar{\bar{G}}_S \cdot \bar{J} \tag{1}$$

and

$$\bar{J} = \bar{\bar{\chi}} \cdot \left(\bar{E}^{\mathrm{i}} + \bar{\bar{G}}_D \cdot \bar{J}\right) \tag{2}$$

where $\bar{E}^{\mathrm{sca}}$ and $\bar{E}^{\mathrm{i}}$ denote the scattered and incident fields, respectively, $\bar{\bar{G}}_S$ and $\bar{\bar{G}}_D$ denote the matrices of Green's function that relate the observation point and the imaging domain and any two points in the imaging domain, respectively. $\bar{J} = \bar{\bar{\chi}} \cdot \bar{E}$ denotes the induced current source, where $\bar{\bar{\chi}}$ and $\bar{E}$ are contrast matrix and the total electric field, respectively [5].

In TWI problems, the wall can be treated as either a part of the background or a part of the target. In the former case, $\bar{\bar{G}}_S$ and $\bar{\bar{G}}_D$ should to be chosen as inhomogeneous (inhomo) background Green's functions. Otherwise they should be chosen as homogeneous (homo) background Green's functions. In any CSI-like algorithm, $\bar{\bar{\chi}}$ and $\bar{J}$ are updated alternatively [3]. If the target and the wall are known to be separable, this priori information can be directly used. In [6], this problem is termed as a 'separable obstacle problem' (SOP). Otherwise it can be considered as an 'obstacle problem' (OP), where the wall-object complex is considered as the scatterer. Under these circumstances, the inversions can be classified into different types according to the used Green's function and whether the case is SOP or OP. In this Letter, these scenarios are denoted as OP-homo, SOP-homo, OP-inhomo and SOP-inhomo, respectively.

In this work, the standard TSOM described in [5] is used to solve the OP-homo problem, where $\bar{\bar{\chi}}$ is updated using a least square method. In solving the SOP-homo problem, the elements in $\bar{\bar{\chi}}$ that reflect the priori information of the wall would remain unchanged during the update [6]. In solving the OP-inhomo problem, we used a method of moment to numerically calculate the Green's function for the inhomogeneous background due to the wall. The process is similar to that reported in [7]. In the calculation, the imaging domain is meshed into 60×60 grids to calculate the $\bar{\bar{G}}_S$ and $\bar{\bar{G}}_D$ values. Finally, the SOP-inhomo problem can be solved based on the OP-inhomo approach by considering the priori information in $\bar{\bar{\chi}}$.

Experiment: In this work, we establish an experimental setup for two-dimensional TWIs with transverse magnetic incidence. Figs. 1*a* and *b* show the schematic diagram and the implemented experimental setup. The system is designed to work at 2.4 GHz. 24 regular patch antennas linearly polarised along the vertical direction are evenly distributed on a circle with a diameter of 113 cm. One of the antennas works as the emitting antenna, which is connected to Port 1 of an Agilent 8722ES vector network analyser (VNA). The others work as receiving antennas, each connected to an output port of a 1-to-23 microwave switching board. The board is implemented with multiple integrated microwave switches (Hittite HMC321LP4). The input port of the microwave switching board is connected to Port 2 of the VNA. Controlled by a micro-controller (Atmel ATmega88), each receiving antenna can be switched to the VNA. By switching the receiving antennas, we can measure the scattered field at different angles.

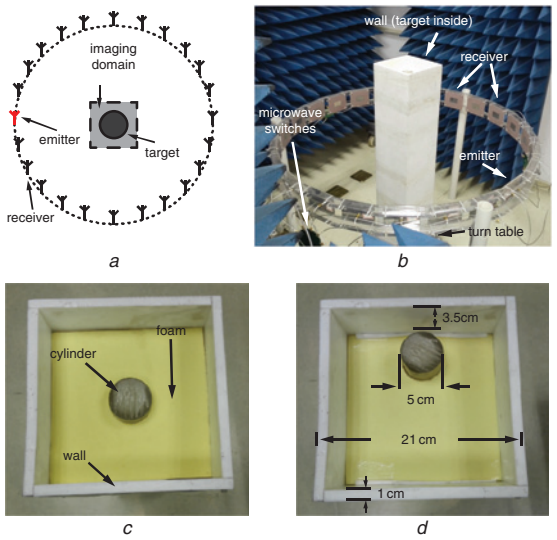

Fig. 1 *Experimental setup*
a Schematic diagram of experimental setup
b Photograph of experimental setup
c Photograph of wall and centred cylinder
d Photograph of wall and off-centred cylinder

Figs. 1*c* and *d* show the configuration of the imaging domain. A 100-cm-long organic glass cylinder is used as the object, whose dielectric constant is around 3. Four Teflon boards with the same length of 100 cm and a dielectric constant of around 2.1 are used to construct the wall. Microwave foams with a close-to-air dielectric constant are used to fix the cylinder to realise the centred and the off-centred states. Finally, the wall-object complex is placed on a turn table, which is located in the centre of the circle. Thus, by rotating the turn table, the scattered field at different angles of incidence can be measured using the single transmitting antenna.

In the first step of the measurement, the total electric field at the place of each receiver with and without the wall-object complex was individually measured. The measured fields in the absence of the complex can be considered as the incident fields. Then, the turn table was rotated by 30°, and the total electric fields in the presence of the complex were measured. Such rotating and measurement were repeated 11 times. By subtracting the incident fields from the total fields measured in the presence of the complex, a 12×23 matrix related to the scattered fields can be obtained. These scattering data are further calibrated using the 'incidence calibration' method proposed in [8].

After calibration, these data are finally used in the inversion of the imaging domain based on (1) and (2). In the OP- and SOP-inhomo

cases, the inhomogeneous background Green's function due to the existence of the wall should be calculated accordingly.

Inversion results: Fig. 2*a* shows the inversion result in the OP-homo scenario, in which the colour bar indicates the value of the dielectric constant, and the dashed lines show the actual profiles of the wall and the object. It is seen that the location, shape, size and dielectric constant of the cylinder can be retrieved from the measured scattering data. However, the shape and the dielectric constant of the wall are quite different from the original ones. The main reason is that the OP-homo inversion does not make full use of the priori information of the wall. Fig. 2*b* shows the inversion result in the SOP-homo scenario. It is seen that with the use of the priori information of the wall, the imaging quality is improved. However, the imaging quality is inferior to those in Figs. 2*c* and *d*, where OP-inhomo and SOP-inhomo inversions are used. This can be explained from the view of the non-linearity of the model. In [6], it is indicated that when the homogeneous background Green's function is used in TWI problems, the non-linearity of the model is stronger than that when an inhomogeneous background Green's function is used. Therefore, in experimental TWIs when measured scattering data are used, the imaging quality based on a homogeneous background Green's function could be deteriorated due to non-ideal factors that do not exist in numerical simulations.

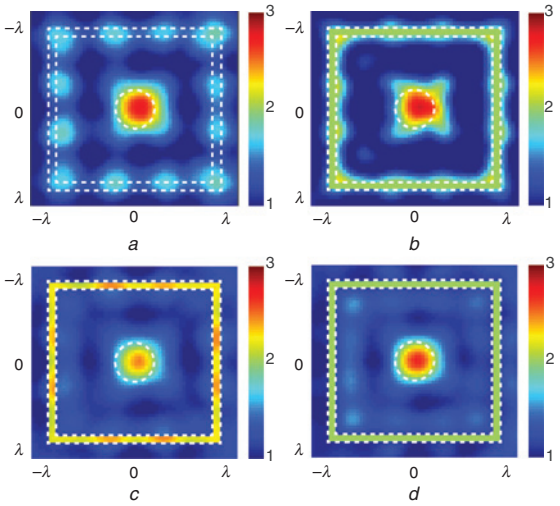

Fig. 2 *Inversion results using experimental data of centred cylinder*
a Inversion result by OP-homo
b Inversion result by SOP-homo
c Inversion result by OP-inhomo
d Inversion result by SOP-inhomo

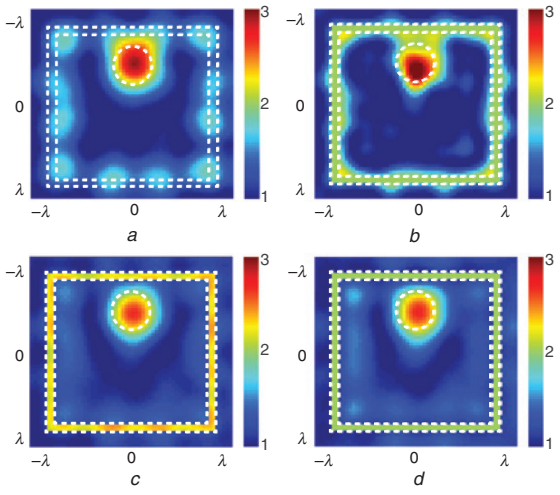

Fig. 3 *Inversion results using experimental data of off-centred cylinder*
a Inversion result by OP-homo
b Inversion result by SOP-homo
c Inversion result by OP-inhomo
d Inversion result by SOP-inhomo

Using the same methods, measurements for an off-centred cylinder were conducted. Compared with the previous case, the only change is that the cylinder is moved to an off-centre place 3.5 cm from one side of the wall. The inversion results are shown in Fig. 3. It can be seen that the inversions based on the inhomogeneous background Green's function are not only able to produce better results, but also able to distinguish the cylinder from the wall.

Conclusion: We have experimentally investigated the TWI with a closed wall based on non-linear TSOM algorithms in four different scenarios. A cost-effective setup is designed and implemented to experimentally test the performance and effectiveness of these methods. The results show that the location, shape, size, and dielectric constant of the object can be retrieved from the measured scattering data, and the SOP-inhomo-based methods are able to generate better imaging results. These imply the potential of TWI for practical applications.

Acknowledgments: This work was supported by the NSFC under grants 61131002, 61528104, 61471315 and 61071063.

Submitted: *18 July 2016* E-first: *12 October 2016*
doi: 10.1049/el.2016.2635
One or more of the Figures in this Letter are available in colour online.

Qingyang Meng, Dexin Ye, Jiangtao Huangfu and Lixin Ran (*Laboratory of Applied Research on Electromagnetics (ARE), Zhejiang University, Hangzhou 310027, People's Republic of China*)

✉ E-mail: ranlx@zju.edu.cn

Changzhi Li (*Department of Electrical and Computer Engineering, Texas Tech University, TX 79409, USA*)

References

1 Ferris, D.D., and Currie, N.C.: 'Survey of current technologies for through-the-wall surveillance (TWS)', *Proc. SPIE*, 1999, **3577**, pp. 62–72, doi: 10.1117/12.336988
2 Soldovieri, F., Solimene, R., and Prisco, G.: 'A multiarray tomographic approach for through-wall imaging', *Trans. Geosci. Remote Sens.*, 2008, **46**, (4), pp. 1192–1199, doi: 10.1109/TGRS.2008.915754
3 Song, L.P., Yu, C., and Liu, Q.H.: 'Through-wall imaging (TWI) by radar: 2-D tomographic results and analyses', *Trans. Geosci. Remote Sens.*, 2006, **43**, (12), pp. 2793–2798, doi: 10.1109/TGRS.2005.857914
4 Abubakar, A., Hu, W., Berg, P.M.V.D., and Habashy, T.M.: 'A finite-difference contrast source inversion method', *Inverse Probl.*, 2008, **24**, (6), pp. 65004–65020, doi: 10.1088/0266-5611/24/6/065004
5 Zhong, Y., and Chen, X.: 'Twofold subspace-based optimization method for solving inverse scattering problems', *Inverse Probl.*, 2009, **25**, (8), pp. 85003–85013, doi: 10.1088/0266-5611/25/8/085003
6 Ye, X., Song, R., Agarwal, K., and Chen, X.: 'Electromagnetic imaging of separable obstacle problem', *Opt. Express*, 2012, **20**, (3), pp. 2206–2219, doi: 10.1364/OE.20.002206
7 Chen, X.: 'Subspace-based optimization method for inverse scattering problems with an inhomogeneous background medium', *Inverse Probl.*, 2010, **26**, (7), pp. 1396–1398, doi: 10.1088/0266-5611/26/7/074007
8 Litman, A., Geffrin, J.M., and Tortel, H.: 'On the calibration of a multistatic scattering matrix measured by a fixed circular array of antennas', *Progr. Electromagn. Res.*, 2010, **110**, (4), pp. 1–21, doi: 10.2528/PIER10090302